IEEE Access
Multidisciplinary | Rapid Review | Open Access Journal

Received March 24, 2021, accepted April 12, 2021, date of publication April 19, 2021, date of current version April 28, 2021.

Digital Object Identifier 10.1109/ACCESS.2021.3073985

Hydro-Dynamic Model and Low-Speed Stability Analysis of Hydraulic Transformer

QIANQIAN BAO, JUNJIE ZHOU, CHONGBO JING, TIANRUI LI, AND MIAOMIAO WANG
School of Mechanical Engineering, Beijing Institute of Technology, Beijing 100081, China

Corresponding author: Junjie Zhou (bit_zhou50082@163.com)

This work was supported by the China Ordnance Group Joint Funding under Grant 6141B012877.

ABSTRACT Hydraulic transformer is a significant component to develop the future energy saving hydraulic systems; however, the speed stability is one of the problems in such a machine because the rotor is unconstrained and the rotary inertia of the rotor is small. In this paper, aiming at the rotating speed of hydraulic transformer, a hydro-dynamic model of is proposed considering the nonlinear friction, oil compressibility and leakage. Both simulation and experiment are carried out to validate the hydro-dynamic model. Moreover, this paper theoretically analyzes the low-speed stability of hydraulic transformer based on the hydro-dynamic model for the first time. The mechanism of creep is discussed and the creep judgment method is presented. The influence of each parameter on creep is investigated, and the possible ways to avoid creep are explored. The calculations of the lowest stable rotating speed and the lowest stable flow rate without creep are given. This study is significant for the design and practical application of hydraulic transformer in the future.

INDEX TERMS Hydraulic transformer, hydro-dynamic model, low-speed stability, creep.

I. INTRODUCTION

Nowadays, with the implementation of global energy conservation and emission reduction strategy, hydraulic transmission system is also required to improve efficiency, and increase flexibility and functionality [1], [2]. Under this condition, as a power conversion unit, hydraulic transformer becomes an universally interesting topic due to the advantages of no throttling loss, energy saving and high efficiency [3], [4].

Hydraulic transformer is firstly proposed by Tyler in 1965 [5]. From then, it roughly experienced the development process from the traditional series structure [6], [7] to the new integrated structure [8], [9], and then to complex improved structures [10]–[12]. The new integrated hydraulic transformer is the mainstream of research, and it can be divided into valve plate rotating type, swash plate rotating type, and composite rotating type (both valve plate and swash plate) according to the adjusting method of control angle [13]. The valve plate rotating hydraulic transformer is firstly invented by Achten in 1997 [14]; however, the pressure ratio of this hydraulic transformer is small due to the limitation of structure [15]–[19]. Then, in terms of this issue, in 2009, our group proposed a swash plate rotating hydraulic transformer with fixed valve plate and the output pressure can be changed by rotating the swash plate [20], which is considered with good potentials to extend pressure ratio in a wide operating condition [21].

However, at present, the research on hydraulic transformer mainly focuses on basic characteristics, such as pressure ratio, efficiency and energy saving application [22], [23], and the research on stability and reliability is very limited, which is an important reason why it has not been widely manufactured and used.

Because the rotor of hydraulic transformer is unconstraint and the rotary inertia of the rotor is small, the rotating speed of hydraulic transformer is greatly affected by the change of torque [24], [25]. Especially, when the rotating speed is low, the friction torque changes greatly, and the rotor of hydraulic transformer is easy to destabilize and creep [26], thus leading to unstable output pressure and output flow rate and even the damage of friction pair in hydraulic transformer. Hence, the stability of transformer is the premise of stable motion of actuator, and the study on rotating speed stability is very important for the maturity of hydraulic transformer.

However, in previous studies, most of researchers study the performance of actuator and the influence of rotating speed

The associate editor coordinating the review of this manuscript and approving it for publication was Zheng Chen.

on the pressure ratio [12], [27], and little attention is paid to rotating speed itself. In terms of system control, some models have been proposed before [24], [28], [29]. On the one hand, these models aims at the whole hydraulic system including hydraulic transformer and actuator, and the rotating speed of hydraulic transformer is just an intermediate variable. In order to simplify the analysis of the control method, the model of hydraulic transformer is simplified to a certain extent, and the factors considered are not comprehensive. On the other hand, these models assume that the transformer has good performance and will not creep. In terms of creep, based on the test phenomenon, Harbin Institute of Technology briefly infers that the reason for creep is the change of torque [30]. However, it does not further discuss the reason for the change of torque and how to avoid creep.

In this work, considering the nonlinear friction, oil compressibility and leakage, a hydro-dynamic model is proposed and validated by simulation and experiment. In addition, low-speed stability of hydraulic transformer is theoretically analyzed based on the hydro-dynamic model for the first time. The critical condition, the mechanism, and the judgment method of creep are discussed. The influence of each parameter on creep is investigated, the possible ways to avoid creep are explored, and the calculations of the lowest stable speed and the lowest stable flow rate without creep are given.

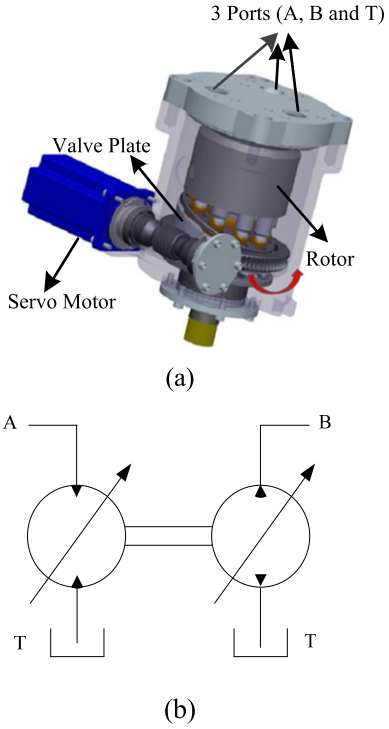

FIGURE 1. Hydraulic transformer: (a) Structure Diagram; (b) Schematic diagram.

II. HYDRO-DYNAMIC MODEL

The hydro-dynamic model indicates the coupling of the hydraulic and dynamic effects in the hydraulic transformer. The hydraulic effects include the torque caused by the pressure ports, the friction exerted on the rotor and flow rate in the outlet port. The dynamic effects mainly indicate the torque balance and speed equation of rotor.

A. DESCRIPTION OF HYDRAULIC TRANSFORMER

Hydraulic transformer is similar to hydraulic pump or motor in structure. The main difference is that the valve plate of hydraulic pump or hydraulic motor has two ports (A and T), while that of hydraulic transformer has three ports (A, B and T). They are linked to high pressure, load, and low pressure, respectively. The combination of port A and T can be considered as a variable motor to rotate the rotor, and the combination of port B and T can be assumed as a variable pump to drive the load. The structure of swash plate-rotating hydraulic transformer and the schematic diagram of hydraulic transformer are shown in Figure 1.

B. TORQUE MODEL

Suppose that V_A, V_B and V_T are the displacement of port A, B and T, respectively, and they can be expressed as [20]:

$$\begin{cases} V_A = 2 \cdot \dfrac{\pi d^2}{4} NR \sin \dfrac{\alpha_A}{2} \sin\delta \tan\gamma \\ V_B = -2 \cdot \dfrac{\pi d^2}{4} NR \sin \dfrac{\alpha_B}{2} \sin(\dfrac{\alpha_T}{2} + \delta) \tan\gamma \\ V_T = 2 \cdot \dfrac{\pi d^2}{4} NR \sin \dfrac{\alpha_T}{2} \sin(\dfrac{\alpha_B}{2} - \delta) \tan\gamma \end{cases} \tag{1}$$

where δ is the rotation angle of swash plate, γ is the inclination angle of swash plate, α_A, α_B, and α_T are the effective wrap angles of port A, B, and T respectively, N is the number of piston, d is the diameter of piston, and R is the reference circle diameter of cylinder block.

Theoretical output torque of port A-T (motor) can be calculated as:

$$T_A = \frac{(P_A - P_T)|V_A|}{2\pi} \tag{2}$$

where P_A is the pressure of port A and P_T is the pressure of port T.

Theoretical input torque of port B-T (pump) can be calculated as:

$$T_B = \frac{(P_B - P_T)|V_B|}{2\pi} \tag{3}$$

where P_B is the pressure of port B.

C. NONLINEAR FRICTION MODEL

The nonlinear friction model adopted in this paper is coulomb friction model [31], as shown in Figure 2. It is assumed that the rotor is only subject to coulomb friction torque after it overcomes the maximum static friction torque, and viscous friction torque is linearly proportional to the angular velocity.

Coulomb friction torque can be expressed as:

$$T_c = \frac{C_f(P_A - P_T)|V_A| + C_f(P_B - P_T)|V_B|}{2\pi} \tag{4}$$

where C_f is the mechanical friction torque loss coefficient.

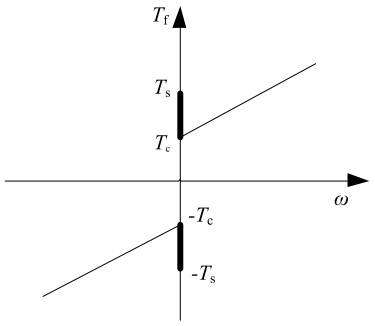

FIGURE 2. The relationship between friction torque and angular velocity in nonlinear friction model.

Viscous friction torque is given as follows:

$$T_d = \frac{C_d \mu \omega \left(|V_A| + |V_B|\right)}{2\pi} \tag{5}$$

where C_d is the viscous friction torque loss coefficient, μ is the dynamic viscosity of the oil and ω is the angular velocity of rotor.

The mathematical formula of coulomb friction model can be expressed as:

$$T_f = \begin{cases} T_s & \omega = 0, \quad \dot{\omega} = 0 \\ C_f(P_A V_A + P_B|V_B|)/2\pi & \omega = 0, \quad \dot{\omega} \neq 0 \\ \left[C_f(P_A V_A + P_B|V_B|) + C_d u \omega (V_A + |V_B|)\right]/2\pi, & \omega \neq 0, \dot{\omega} \neq 0 \end{cases} \tag{6}$$

where T_s is maximum static friction torque.

D. FLOW RATE MODEL

The theoretical flow rate of port B is given as follows:

$$Q_{Bth} = \frac{\omega}{2\pi}|V_B| \tag{7}$$

The leakage flow rate of port B is given as follows:

$$Q_S = \frac{C_s}{2\pi u}|V_B|P_B \tag{8}$$

where C_s is laminar leakage coefficient.

The compression flow rate of port B is given by:

$$Q_C = \beta V_0 \frac{dP_B}{dt} \tag{9}$$

where V_0 is the fluid volume in the hydraulic transformer and pipeline before the transformer starts, and β is the oil compressibility coefficient.

Then, the actual flow rate of port B can be derived as:

$$Q_B = Q_{Bth} - Q_S - Q_C = \frac{\omega}{2\pi}|V_B| - \frac{P_B C_s}{2\pi\mu}|V_B| - \beta V_0 \frac{dP_B}{dt} \tag{10}$$

This flow rate model takes account of leakage and the compressibility of the oil.

E. ROTATING ANGULAR VELOCITY MODEL

The transformer rotates under the combined function of input torque, output torque and nonlinear friction torque, then:

$$T_A - T_B - T_f = J\dot{\omega} \tag{11}$$

where J is the rotary inertia of rotor.

Suppose that $P_T = 0$, so the torque balance equation can be obtained by:

$$\frac{|V_A|}{2\pi}P_A - \frac{|V_B|}{2\pi}P_B - \frac{C_f(P_A V_A + P_B|V_B|)}{2\pi} - \frac{C_d \mu \omega (V_A + |V_B|)}{2\pi} = J\dot{\omega} \tag{12}$$

By combining the Eq. (10) and the Eq. (12), the angular velocity equation can be obtained as follows:

$$\ddot{\omega} + \left(\frac{C_s|V_B|}{2\pi\mu\beta V_0} + \frac{C_d\mu\left(|V_A| + |V_B|\right)}{2\pi J}\right)\dot{\omega} + \frac{|V_B|^2(1 + C_f) + C_d C_s\left(|V_A| + |V_B|\right)|V_B|}{4\pi^2 J\beta V_0}\omega = \frac{|V_B|(1 + C_f)}{2\pi J\beta V_0}Q_B + \frac{|V_A||V_B|P_A(1 - C_f)C_s}{4\pi^2 J\mu\beta V_0} \tag{13}$$

Suppose that the flow rate at port B jumps from 0 to Q_B and the pressure at port A jumps from 0 to P_A at start time.

From the Eq. (6), we can obtain the boundary condition as follows:

$$\dot{\omega} = \frac{T_s - T_c}{J}, \quad \omega = 0 \tag{14}$$

Suppose that:

$$\omega_n = \sqrt{\frac{|V_B|^2(1 + C_f) + C_d C_s\left(|V_A| + |V_B|\right)|V_B|}{4\pi^2 J\beta V_0}} \tag{15}$$

$$\zeta = \frac{\frac{C_s|V_B|}{u\beta V_0} + \frac{C_d\mu(|V_A| + |V_B|)}{J}}{2\sqrt{\frac{|V_B|^2(1 + C_f) + C_d C_s(|V_A| + |V_B|)|V_B|}{J\beta V_0}}} \tag{16}$$

$$\omega_0 = \frac{\frac{|V_B|(1 + C_f)}{2\pi J\beta V_0}Q_B + \frac{|V_A||V_B|P_A(1 - C_f)C_s}{4\pi^2 J\mu\beta V_0}}{\frac{|V_B|^2(1 + C_f) + C_d C_s(|V_A| + |V_B|)|V_B|}{4\pi^2 J\beta V_0}} \tag{17}$$

where ζ is the damping ratio of hydraulic transformer, ω_n is the undamped natural frequency of hydraulic transformer, and ω_0 is the stable-state angular velocity of the hydraulic transformer.

From the above three equations, it can be seen that ζ and ω_n are only related to the structure of hydraulic transformer itself and reflect the inherent property of hydraulic transformer. ω_0 is related not only to the structure of hydraulic transformer itself but also to the input of hydraulic transformer (Q_B and P_A).

Then, the Eq. (13) can be simplified as:

$$\ddot{\omega} + 2\zeta\omega_n\dot{\omega} + \omega_n^2\omega = \omega_n^2\omega_0 \tag{18}$$

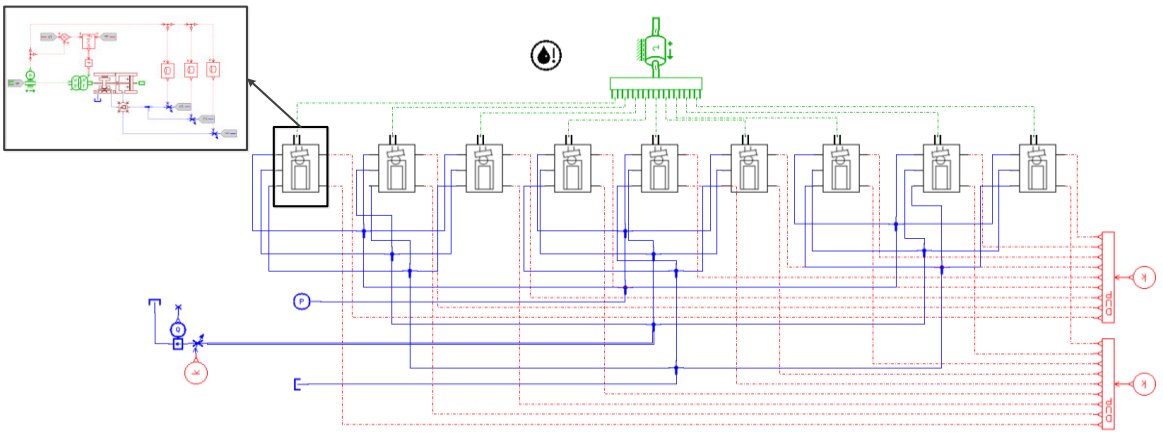

FIGURE 3. The simulation model of hydraulic transformer in AMESim.

TABLE 1. Parameters of the transformer.

Parameter	Value	Parameter	Value
C_d	191974	$\gamma(^\circ)$	18
C_s	2.2746*10^{-8}	V_0(m^3)	1*10^{-4}
C_f	0.0272	β(pa^{-1})	0.67*10^{-9}
μ(pa*s)	0.03	J(kgm^2)	0.01
d(mm)	22.18	R(mm)	49.3
coefficient of viscous friction(Nm/(rev/min))	0.04	T_c (Nm)	5

By taking the Laplace transform of the above equation, Eq. (14) can be rewritten as:

$$\left[s^2\omega(s) - sw(0) - \dot{w}(0)\right] + 2\zeta\omega_n\left[s\omega(s) - w(0)\right] + w_n^2\omega(s) = \omega_n^2\omega_0\frac{1}{s}$$

Substitute the boundary condition (Eq. (14)) into the above equation, and we can obtained that:

$$s^2\omega(s) + 2\zeta\omega_n s\omega(s) + w_n^2\omega(s) = \omega_n^2\omega_0\frac{1}{s} + \frac{T_s - T_c}{J} \quad (19)$$

It can be seen from the above equation that the angular velocity is the sum of the response under the step and impulse input.

When $0 < \zeta < 1$, the angular velocity of hydraulic transformer is calculated as follows:

$$\omega(t) = \omega_0\left[e^{-\zeta\omega_n t}\left(-\frac{\zeta}{\sqrt{1-\zeta^2}}\sin\omega_d t - \cos\omega_d t\right) + 1\right] + \frac{T_s - T_c}{J\omega_d}e^{-\zeta\omega_n t}\sin\omega_d t \quad (20)$$

where ω_d is the damped natural frequency of hydraulic transformer and $\omega_d = \omega_n\sqrt{1-\zeta^2}$.

When $\zeta = 1$, the angular velocity is as follows:

$$\omega(t) = \frac{T_s - T_c}{J}\left[1 - (1+\omega_n t)e^{-\omega_n t}\right] + \omega_0\omega_n^2 t e^{-\omega_n t} \quad (21)$$

When $\zeta > 1$, the angular velocity is calculated as follows:

$$\omega(t) = \frac{\omega_n\omega_0}{2\sqrt{\zeta^2-1}}\left[e^{-\left(\zeta-\sqrt{\zeta^2-1}\right)\omega_n t} - e^{-\left(\zeta+\sqrt{\zeta^2-1}\right)\omega_n t}\right] + \frac{T_s - T_c}{J}\left[1 - \frac{e^{-(\zeta-\sqrt{\zeta^2-1})\omega_n t}}{2(1+\zeta\sqrt{\zeta^2-1}-\zeta^2)} - \frac{e^{-(\zeta+\sqrt{\zeta^2-1})\omega_n t}}{2(1-\zeta\sqrt{\zeta^2-1}-\zeta^2)}\right] \quad (22)$$

III. SIMULATION AND EXPERIMENT VALIDATION

A. SIMULATION WITH AMESim

Taking the swash plate-rotating hydraulic transformer developed and designed by our laboratory (see Figure 1(a)) as an example, the simulation is conducted in AMESim. The coulomb friction model is also used in the friction model of rotor, which is consistent with the theory. The simulation model is shown in Figure 3 and the basic parameters [32] are shown in Table 1.

B. EXPERIMENTAL PLATFORM

The principle and apparatus of the experimental platform are shown in Figure 4. The three oil ports of hydraulic transformer are connected with constant pressure pump, load and tank, respectively. The constant pressure pump is used to simulate the high pressure of the constant pressure network, and the throttle valve can be regarded as load. The hardware devices used in the test are shown in Table 2.

C. RESULTS AND DISCUSSION

1) MAXIMUM STATIC FRICTION TORQUE

Set δ and the opening of throttle valve as constant, and start the constant pressure pump. Because the sampling mode of

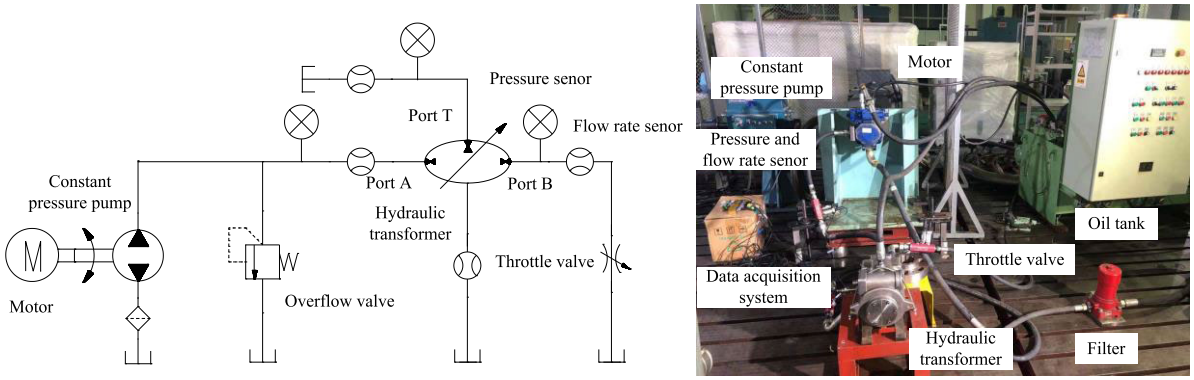

(a) (b)

FIGURE 4. Experimental platform: (a) Experiment principle; (b) Experiment apparatus.

TABLE 2. Details of hardware devices in the experiment of hydraulic transformer.

Name	Specification	Quantity	Remark
Speed encoder	OVW-2	1	Measure the speed of transformer
Pressure sensor	JYB/40MPa	3	Measure the pressure of three oil ports
Flow sensor	EVS3100-1	3	Measure the flow rate of three oil ports
Data acquisition system	Dewesoft	1	Obtain test data

TABLE 3. Datas of hydraulic transformer the moment before start.

Serial number	δ (°)	P_A (MPa)	P_B (MPa)	P_T (MPa)	T_s (N*m)
1	45	3.2	0.61	0.97	29.556
2	72	2.48	0.19	1.08	30.605

data acquisition equipment is discrete, the experimental data just right at the start moment of hydraulic transformer is not easy to collect. So we use the data before the start moment to approximate the data just right at the start moment. Pressures of three ports are shown in Table 3 respectively. Then the maximum static friction torque can be expressed as follows:

$$T_s = \frac{(P_A - P_T)V_A - V_B(P_B - P_T)}{2\pi}$$

Averaging the calculated maximum static friction torque, we can obtain that the value of maximum static friction torque is 30.1 N*m.

2) ROTATING SPEED

Set δ and the opening of throttle valve as constant, and start the constant pressure pump. Then, record the rotating speed of the hydraulic transformer from start to stable operation. Set the parameters of theory and simulation to be consistent with the experiment. The results are shown in Figure 5.

The results of theory, simulation and experiment are shown in Table 4 and Table 5. By comparing these data, the following conclusions can be summarized:

(1) The stable rotating speed of theory is slightly greater than that of simulation, and the stable rotating speed of simulation is slightly greater than that of experiment. The stable rotating speed of simulation is close to that of simulation, and the error is only 4%.

(2) The stable rotating speed of theory is also close to that of experiment. The error between them is 13.9% when $Q_B = 26$L/min, and it is 10.1% when $Q_B = 40$L/min. Consequently, the average error is about 12.5%, which verify the accuracy of hydro-dynamic model to some extent. The error is mainly caused by the simplification of the model, the measurement error of J, C_d, C_f, C_s, T_s and the leakage of hydraulic transformer.

(3) The rotating speed of theory and simulation both have overshoot relative to the stable rotating speed. The maximum rotating speed of theory is close to that of simulation. The error between them is 7.9% when $Q_B = 26$L/min, and it is 19.2% when $Q_B = 40$L/min. Therefore, the average error is about 13.55%, which verify the correctness of hydro-dynamic model to a certain extent. In addition, the response speed of theory is faster than that of simulation. The errors of maximum rotating speed and response speed are mainly caused by the difference between theory and simulation model. The theory model is not considered the plunger distribution; however, it is taken into account in simulation model.

(4) The output pressure of constant pressure pump is determined by the flow rate, and it cannot reach the set value immediately at start moment. In addition, the leakage of hydraulic transformer is a little large. Therefore, the response speed of hydraulic transformer is slower in the test, and the rotating speed has no overshoot.

(5) Because the non-uniformity caused by the pistons is not taken into account in the hydro-dynamic model, the pulsation of rotating speed of theory model is smaller than that of simulation and experiment.

TABLE 4. Comparison of theory, simulation and experiment results (stable state).

Serial number	Theory stable rotating speed (r/min)	Simulation stable rotating speed (r/min)	error	Test stable rotating speed (r/min)	error
1	274	262	4.4%	236	13.9%
2	577	550	4.7%	519	10.1%

TABLE 5. Comparison of theory and simulation results (dynamic state).

Serial number	Maximum rotating speed (r/min)		
	Theory	Simulation	error
1	441	476	7.9%
2	739	597	19.2%

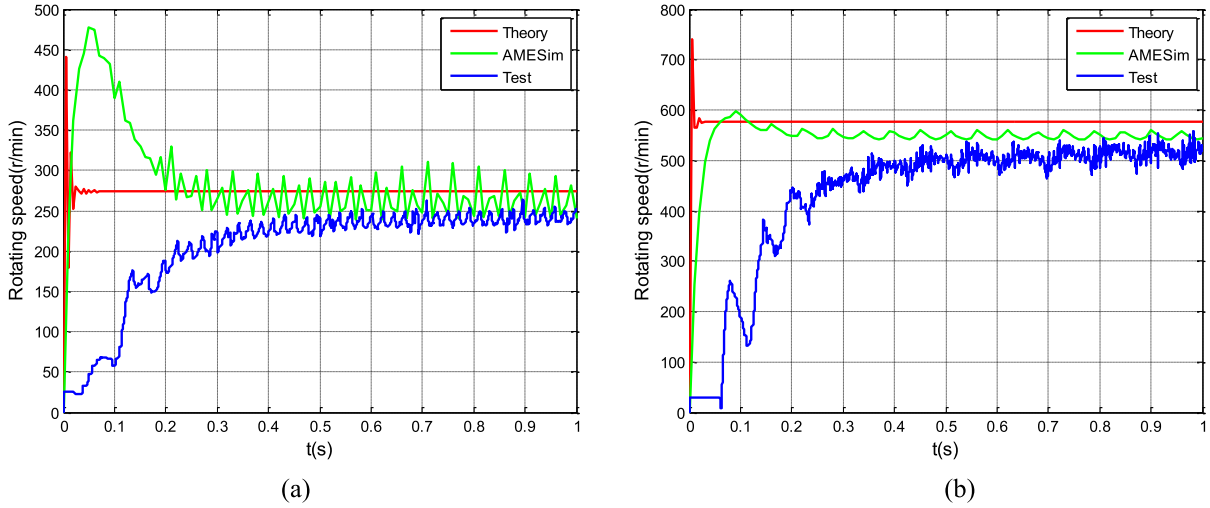

FIGURE 5. Rotating speed of hydraulic transformer: (a) Results of theory, simulation, and test when QB = 26L/min; (b) Results of theory, simulation, and test when QB = 40L/min.

TABLE 6. Operating angular velocity under impulse input and step input.

ζ	AVR1	AVR2	Σ(AVR1+ AVR2)
$\zeta \leq 0$	×	×	×
$0<\zeta<1$	+/-	+	+/-
$\zeta \geq 1$	+	+	+

Note: AVR1 means angular velocity of hydraulic transformer under impulse input. AVR2 means angular velocity of hydraulic transformer under step input. Symbol × means the hydraulic transformer cannot run stably. Symbol + means positive value and symbol - means negative value.

IV. LOW SPEED STABILITY

Low speed stability is an important factor that affects the working performance of hydraulic transformer. Hydraulic transformer is easy to creep when its speed is low, and the creep is an important index to judge its low-speed stability.

A. CRITICAL CONDITION FOR CREEP

When the rotating speed of hydraulic transformer is low, hydraulic transformer usually cannot maintain stable rotating speed, and enters an unstable motion of start/stop sequences, which is called the creep of hydraulic transformer. Thus, if the creep occurs, the rotating speed must be 0 at a certain moment.

Based on the value of ζ, the sign of angular velocity is discussed as follows (see Table 6):

- When $\zeta < 0$, the angular velocity under both step input and impulse input are all oscillatory; thus, the hydraulic transformer cannot run stably and the study does not make sense.
- When $\zeta = 0$, the angular velocity under both step and impulse input are all persistent oscillation; therefore, the hydraulic transformer also cannot run stably and the study does not make sense.
- When $\zeta \geq 1$, the angular velocity under step input and under pulse input are all positive; consequently, the sum of angular velocity is also positive and creep is impossible.
- When $0< \zeta < 1$, the angular velocity is positive under step input, and it may be negative under impulse input; thus, the sum of angular velocity may be negative and creep may occur.

So the necessary condition for creep is $0 < \zeta < 1$.

Figure 6 shows the change of angular velocity after hydraulic transformer starts. The curve (a) represents that the hydraulic transformer does not creep, the curve (c) indicates that the hydraulic transformer creeps, and the curve (b) shows

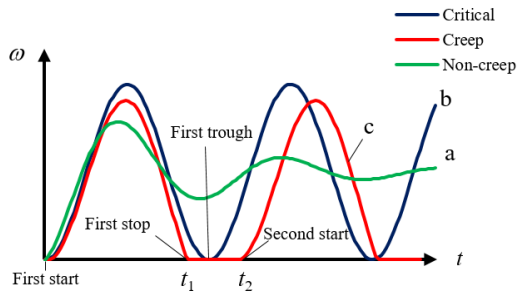

FIGURE 6. Change of angular velocity of hydraulic transformer. Note: t_1 and t_2 are the moment of first stop and second start of hydraulic transformer in the curve (c), respectively.

that the hydraulic transformer is in the critical state between creep and non-creep.

When the curve does not intersect with the t-axis at the first trough, the fluctuation of the angular velocity will gradually decrease and become a stable state (see curve (a)). Assume that $t_2 - t_1$ is the duration from first stop to second start of hydraulic transformer in the curve (c). When $t_2 - t_1$ decreases to 0, the curve (c) is tangent to t-axis and the hydraulic transformer becomes critical state curve (see curve (b)). So whether hydraulic transformer creeps depends on whether the first trough of angular velocity waveform decreases to 0.

Obviously, from the curve (b), we can see that the critical condition of creep is:

$$0 < \zeta < 1, \quad t = t_1,\ \omega = 0,\ \dot{\omega} = 0,\ \ddot{\omega} > 0 \tag{23}$$

When $0 < \zeta < 1$ and the absolute value of the angular velocity under impulse input is greater than that under step input, the sum of angular velocity will be negative and then creep will occur.

B. MECHANISM OF CREEP

As the main working medium of hydraulic transformer, hydraulic oil has compressibility. Hence, the torque generated by the hydraulic oil can be regarded as variable spring torque. Meanwhile, the Eq. (12) changes from first order to second order. This factor provides the condition for the generation of creep.

On the other hand, the friction torque of hydraulic transformer normally increases with the increase of rotating speed. However, in the stationary and low-speed zone, the friction torque decreases with the rise of rotating speed instead. The decrease of friction torque causes the impulse input (Eq. (19)), thus leading to the possible negative values of angular velocity, which promotes the generation of creep. Therefore, the main reasons for the creep of hydraulic transformer are the oil compressibility and the decrease of friction torque in low-speed zone.

The specific process of creep (see Figure 7) is as follows:

(1) When the pressure of constant network reaches the start pressure of hydraulic transformer, the transformer begins to rotate.

(2) The friction torque decreases at start moment.

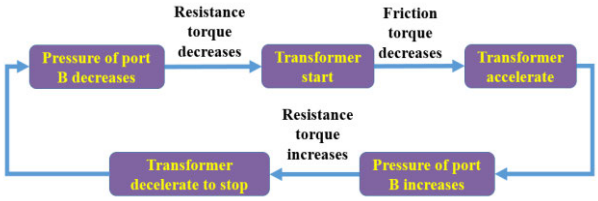

FIGURE 7. Creep process of hydraulic transformer.

(3) The transformer begins to accelerate, and its rotating speed increases.

(4) The flow rate of port B increases (see Eq. (7)), which leads to the increase of pressure of port B (see Eq.(9)).

(5) The resistance torque of transformer generated by port B increases.

(6) The transformer begin to decelerate until it stops.

(7) The flow rate of port B decreases (see Eq. (7)), thus leading to the decrease of pressure in port B (see Eq.(9)).

(8) The resistance torque of transformer generated by port B decreases.

(9) The transformer restarts again and enters into the next running cycle when the pressure of port A reaches the start pressure again.

C. CREEP JUDGMENT METHOD

The curve (b) in Figure 6 shows the critical state of creep, and contains the functional characteristic of creep. So the curve (b) is adopted as a research subject in this part.

Eq. (20) can be expressed as follows:

$$\omega(t) = \left(\frac{T_s - T_c}{J\omega_n} - \omega_0\zeta\right)\frac{1}{\sqrt{1-\zeta^2}}e^{-\zeta\omega_n t}\sin\omega_d t - w_0 e^{-\zeta\omega_n t}\cos\omega_d t + \omega_0 \tag{24}$$

In order to simplify the calculation, suppose that:

$$Z = \frac{J\omega_n\omega_0}{T_s - T_c} \tag{25}$$

Z is named the creep index of hydraulic transformer. $J/(T_s - T_c)$ is the reciprocal of the impulse input, and ω_0 is the stable-state response under step input. Therefore, Z can reflect the common effect of impulse input and step input on the hydraulic transformer.

Then Eq. (24) can be rewritten as:

$$\begin{aligned}\omega(t) &= \left[\frac{1-\zeta Z}{Z\sqrt{1-\zeta^2}}\sin\omega_d t - \cos\omega_d t\right]e^{-\zeta\omega_n t}\omega_0 + \omega_0 \\ &= Ae^{-\zeta\omega_n t}\omega_0\sin(\omega_d t - \theta) + \omega_0\end{aligned} \tag{26}$$

where $A = \sqrt{(1 - 2\zeta Z + Z^2)/(Z^2(1-\zeta^2))}$, and $\tan\theta = Z\sqrt{1-\zeta^2}/(1-\zeta Z)$.

Taking the derivative of Eq. (26) and setting it equal to 0, we can obtain that:

$$\dot{\omega}(t) = -\zeta\omega_n A e^{-\zeta\omega_n t}\omega_0\sin(\omega_d t - \theta) + Ae^{-\zeta\omega_n t}\omega_0\omega_d\cos(\omega_d t - \theta) = 0 \tag{27}$$

Then, we can get that:

$$\tan(\omega_d t - \theta) = \sqrt{1-\zeta^2}/\zeta \tag{28}$$

Further, t can be calculated as:

$$t = (\alpha + k\pi + \theta)/\omega_d \tag{29}$$

where $\alpha = \arctan(\sqrt{1-\zeta^2}/\zeta)$.

Taking the derivative of Eq. (27), we can obtain that:

$$\ddot{\omega}(t) = Ae^{-\zeta\omega_n t}\omega_0\omega_n^2(2\zeta^2-1)\sin(\omega_d t-\theta) - Ae^{-\zeta\omega_n t}\omega_0\omega_n^2 2\zeta\sqrt{1-\zeta^2}\cos(\omega_d t-\theta) \tag{30}$$

When $K = 0$, $t = (\alpha+\theta)/\omega_d$,

$$\ddot{\omega}(t) = Ae^{-\zeta\omega_n t}\omega_0\omega_n^2\sqrt{1-\zeta^2}(-1) < 0 \tag{31}$$

When $K = 1$, $t = (\alpha+\theta)/\omega_d$,

$$\ddot{\omega}(t) = Ae^{-\zeta\omega_n t}\omega_0\omega_n^2\sqrt{1-\zeta^2}(1) > 0 \tag{32}$$

According to the critical condition of creep (Eq. (12)), it is obvious that:

$$K = 1, \quad t_1 = (\alpha+\theta+\pi)/\omega_d$$

Set $t = (\alpha+\theta+\pi)/\omega_d$, and substitute it into Eq. (26). When the hydraulic transformer is in the critical state, it satisfies:

$$e^{-\zeta\frac{\alpha+\theta+\pi}{\sqrt{1-\zeta^2}}} = \frac{Z}{\sqrt{1-2\zeta Z+Z^2}} \tag{33}$$

According to the Eq. (33), the curve with ζ as the abscissa and Z as the ordinate is drawn, as shown in Figure 8. The curve in the figure is called critical line. This critical line divides the running zone into two parts: creep zone (lower part) and non-creep zone (upper part). The value of Z on the critical line is named creep threshold value under this ζ, which is represented by $Z_0(\zeta)$.

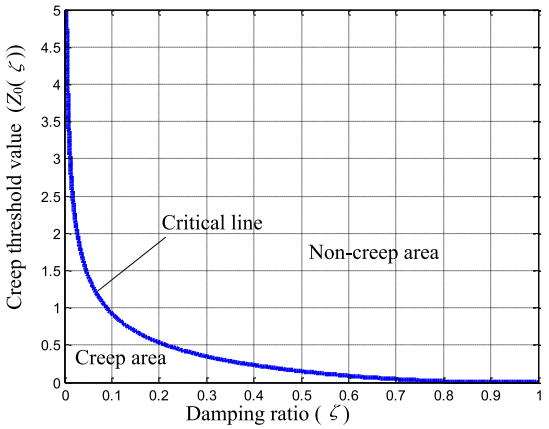

FIGURE 8. ζ–$Z_0(\zeta)$ diagram.

Based on the Figure 8, we can obtain a method to judge whether hydraulic transformer creeps under a certain working condition. Specific steps are as follows:

(1) ζ should be calculated by Eq. (16). Then, the magnitude of ζ should be judged. When $\zeta \geq 1$, transformer does not creep; when $0 < \zeta < 1$, whether transformer creeps is uncertain.

(2) Z should be computed further by Eq. (25) and $Z_0(\zeta)$ should be obtained by Figure 8.

(3) The magnitude of Z and $Z_0(\zeta)$ should be compared. When $Z > Z_0(\zeta)$, transformer does not creep; when $Z < Z_0(\zeta)$, the transformer creeps; when $Z = Z_0(\zeta)$, transformer is in the critical state.

D. INFLUENCE PARAMETERS

1) CREEP THRESHOLD VALUE

ζ is the intrinsic parameter of hydraulic transformer. Figure 8 shows that $Z_0(\zeta)$ is uniquely determined by ζ, and is negatively correlated with ζ. Therefore, $Z_0(\zeta)$ is also the intrinsic parameter of hydraulic transformer. It can be seen from Eq. (16) that ζ is related to J, δ, V_0, β, C_d, C_f, C_s, μ. Therefore, $Z_0(\zeta)$ is also linked to J, δ, V_0, β, C_d, C_f, C_s, μ. The relationships between these parameters and creep threshold value are shown in Figure 9.

Figure 9 shows that $Z_0(\zeta)$ decreases when δ, C_d and C_f increase, respectively, $Z_0(\zeta)$ increases when C_s increases, and $Z_0(\zeta)$ decreases firstly and then increases when J, V_0, β and μ increase, respectively.

In order to reduce creep and achieve good low-speed stability of hydraulic transformer, $Z_0(\zeta)$ should be low. Therefore, C_s should be decreased, δ, C_d and C_f should be increased, and appropriate values of J, V_0, β, μ should be selected.

2) CREEP INDEX

Combining Eq. (15), Eq. (17) and Eq. (25), we can obtain that:

$$Z = \frac{J\omega_n\omega_0}{T_s - T_c} = \frac{J}{T_s-T_c}\frac{\frac{|V_B|(1+C_f)}{2\pi J\beta V_0}Q_B + \frac{|V_A||V_B|P_A(1-C_f)C_s}{4\pi^2 J\mu\beta V_0}}{\sqrt{\frac{|V_B|^2(1+C_f)+C_dC_s(|V_A|+|V_B|)|V_B|}{4\pi^2 J\beta V_0}}} \tag{34}$$

From Eq. (16), Eq. (33) and Eq. (34), we can obtain that $T_s - T_c$ mainly affects Z, not associated with $Z_0(\zeta)$. The relationships between $T_s - T_c$ and Z are shown in Figure 10(a). It can be seen that Z decreases when $T_s - T_c$ increases. Thus, $T_s - T_c$ should be decreased in order to achieve good low-speed stability of the hydraulic transformer.

It can be seen from Eq. (34) that $T_s - T_c$, J, V_0, β, C_d, C_f, C_s, μ, etc. are constant after the hydraulic transformer is designed. So Z is only related to Q_B, P_A and δ when the transformer works. The relationships between Q_B, P_A, δ and creep index are shown in Figure 10(a) and 10(b). It can be seen that Z increases along with the increase of Q_B and P_A, and the effect of Q_B on Z is much greater than that of P_A on Z. Z increases along with the increase of δ.

It can be observed from Figure 8 that the smaller Z is, the more likely it is to creep when ζ is given. Therefore, in order to avoid creep and achieve good low-speed stability

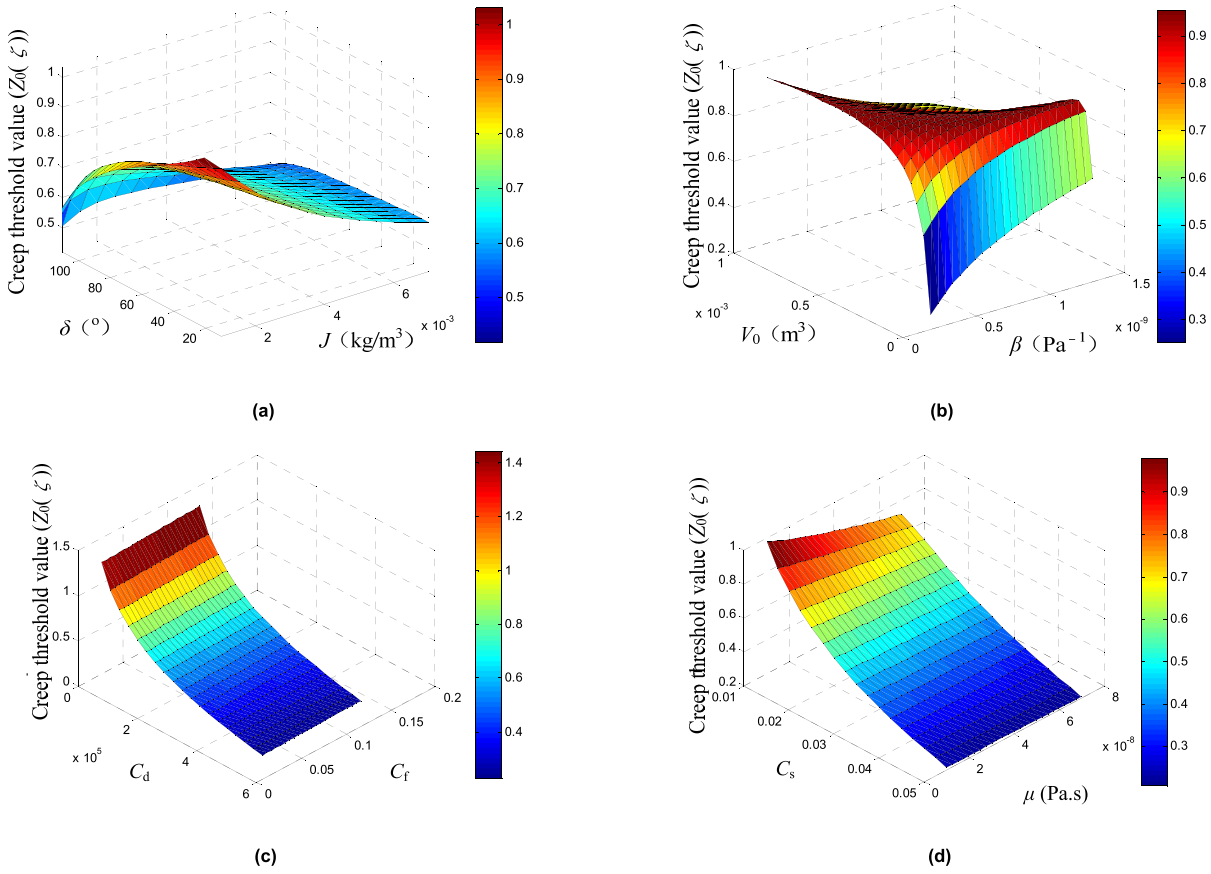

FIGURE 9. Parameter influence on the creep threshold value: (a) δ and J ; (b) β and V_0 ; (c) C_d and C_f ; (d) C_s and μ.

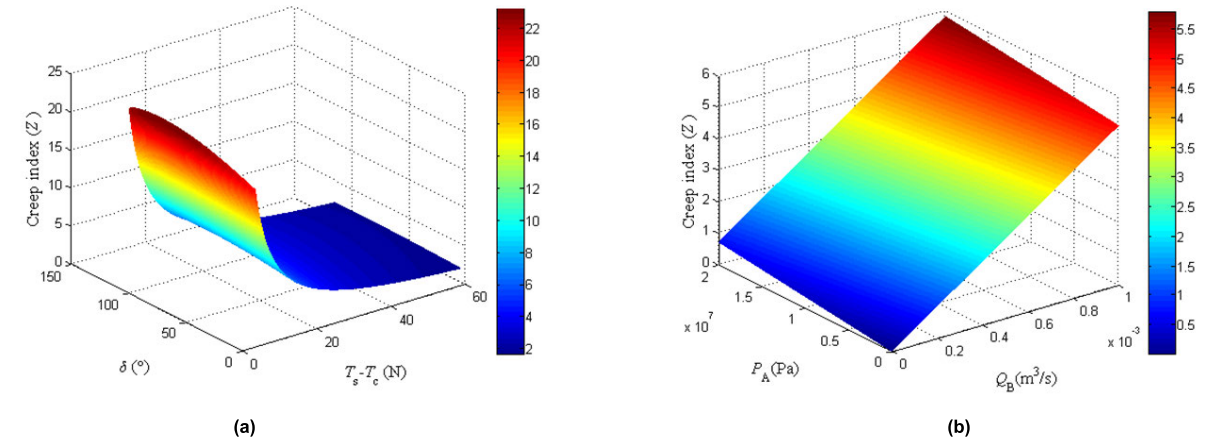

FIGURE 10. Parameter influence on the creep index: (a) δ and T_S-T_C ; (b)P_A and Q_B.

of the hydraulic transformer, Q_B and P_A should be increased. Z and $Z_0(\zeta)$ both increase when δ increases, so appropriate values of δ should be selected.

Through the above analysis, the influence of each parameter on creep threshold value ($Z_0(\zeta)$) and creep index (Z) is obtained. So the parameter collocation of the hydraulic transformer can be estimated when the hydraulic transformer does not creep, which can be used as a reference for component and system design and point out the direction for improving low-speed stability in the future.

E. LOWEST STABLE ROTATING SPEED AND LOWEST STABLE FLOW RATE

The rotating speed when hydraulic transformer just creeps is called the lowest stable rotating speed. When ζ is known, $Z_0(\zeta)$ can be found from Figure 8. Then the lowest stable

rotating speed can be obtained by:

$$\omega_{\mathrm{L}} = \frac{Z_0\left(\zeta\right)\left(T_{\mathrm{s}} - T_{\mathrm{c}}\right)}{J\omega_{\mathrm{n}}} \tag{35}$$

The flow rate of port B corresponding to the lowest stable rotating speed is called the lowest stable flow rate. By substituting ω_{L} into the Eq. (17), the lowest stable flow rate can be calculated as follows:

$$Q_{\mathrm{BL}} = 2\pi\left[|V_{\mathrm{B}}| + \frac{C_{\mathrm{d}}C_{\mathrm{s}}\left(|V_{\mathrm{A}}| + |V_{\mathrm{B}}|\right)}{1 + C_{\mathrm{f}}}\right]\omega_{\mathrm{L}} - \frac{2\pi P_{\mathrm{A}}(1 - C_{\mathrm{f}})C_{\mathrm{s}}|V_{\mathrm{A}}|}{u\left(1 + C_{\mathrm{f}}\right)} \tag{36}$$

If the hydraulic transformer does not creep, the stable rotating speed must be greater than ω_{L}, and the flow rate of port B must be greater than Q_{BL}.

From Eq. (35) and Eq. (36), the lowest stable speed and lowest stable flow rate of hydraulic transformer without creep can be obtained and marked on the nameplate of hydraulic transformer, which is significant for its practical application.

V. CONCLUSION

In order to achieve a strong understanding of the operation of hydraulic transformer, a hydro-dynamic model of hydraulic transformer is proposed considering the nonlinear friction, oil compressibility and leakage. Both simulation and experiment are carried out to validate the hydro-dynamic model. Results show that the theory has a good correlation with both the simulation and the experiment.

The low-speed stability is deeply analyzed based on the hydro-dynamic model. The mechanism of creep is discussed and the method to judge whether the transformer creeps is presented. Analysis shows that the fundamental reason for creep is the compressibility of oil and the decrease of friction torque in low-speed zone. Moreover, the concept of creep threshold value and creep index are proposed, the influence of parameters on these two concepts are analyzed, and the possible ways to avoid creep are explored. In addition, this paper provides the calculation method of the lowest stable rotating speed and the lowest stable flow rate without creep. Future work in this direction can be the study of and improving operation stability of the hydraulic transformer.

NOMENCLATURE

V_{A}	displacement of port A, m^3
V_{B}	displacement of port B, m^3
V_{C}	displacement of port C, m^3
P_{A}	pressure of port A, Pa
P_{B}	pressure of port B, Pa
P_{T}	pressure of port T, Pa
T_{A}	Theoretical output torque of port A-T, N.m
T_{B}	Theoretical output torque of port B-T, N.m
T_{f}	friction torque, N.m
T_{s}	maximum static friction torque, N.m
T_{c}	coulomb friction torque, N.m
T_{d}	viscous friction torque, N.m
Q_{B}	actual flow rate of port B, m^3/s
Q_{Bth}	theoretical flow rate of port B, m^3/s
Q_{S}	leakage flow rate of the port B, m^3/s
Q_{C}	compression flow rate of port B, m^3/s
D	diameter of piston, m
R	reference circle diameter of piston on the cylinder block, m
N	number of piston
α	effective angle of distribution ports; °
δ	rotation angle of swash plate; °
γ	inclination angle of swash plate; °
C_{d}	viscous friction torque loss coefficient
C_{f}	mechanical friction torque loss coefficient
C_{s}	laminar leakage coefficient
β	oil compressibility coefficient; Pa^{-1}
μ	viscosity, Pa·s
V_0	fluid volume in the hydraulic transformer and pipeline, m^3
J	rotational inertia of hydraulic transformer, kg/m^2
ω	angular velocity of hydraulic transformer, rad/s
ζ	damping ratio of the system
ω_{n}	natural angular frequency of the system
Z_0	creep threshold value
Z	creep index

REFERENCES

[1] G. Wu, J. Yang, J. Shang, and D. Fang, "A rotary fluid power converter for improving energy efficiency of hydraulic system with variable load," *Energy*, vol. 195, no. 4, pp. 1–12, Mar. 2020, doi: 10.1016/j.energy.2020.116957.

[2] R. Bao, Q. Wang, and T. Wang, "Energy-saving trajectory tracking control of a multi-pump multi-actuator hydraulic system," *IEEE Access*, vol. 8, pp. 179156–179166, Jan. 2020, doi: 10.1109/ACCESS.2020.3027354.

[3] W. Wu, J. Hu, S. Yuan, and C. Di, "A hydraulic hybrid propulsion method for automobiles with self-adaptive system," *Energy*, vol. 114, pp. 683–692, Nov. 2016, doi: 10.1016/j.energy.2016.08.042.

[4] W. Wu, C. Di, and J. Hu, "Dynamics of a hydraulic-transformer-controlled hydraulic motor system for automobiles," *Proc. Inst. Mech. Eng., D, J. Automobile Eng.*, vol. 230, no. 2, pp. 229–239, Feb. 2016, doi: 10.1177/0954407015583618.

[5] H. P. Tyler, "Fluid intensifier," U.S. Patent 3 188 963, Jun. 15, 1965.

[6] H. K. Herbert, "Hydraulic transformer," U.S. Patent 3 627 451, Dec. 14, 1971.

[7] H. L. Dong, J. H. Jiang, and S. L. Wu, "Research on the optimum conditions and energy recuperating of hydraulic accumulators in series to hydraulic transformer," (in Chinese), *China Mech. Eng.*, vol. 14, no. 3, pp. 192–195, Feb. 2003.

[8] H. Y. Lu, "Theoretical analysis and experiment of electric control bent axial piston hydraulic transformer," Ph.D. dissertation, Harbin Inst. Technol., Harbin, China, 2008.

[9] C. Q. Liu and J. H. Jiang, "The effect of the plunger number on hydraulic transformer's flow pulsation rate," *High Technol. Lett.*, vol. 19, no. 1, pp. 30–36, Mar. 2013, doi: 10.3772/j.issn.1006-6748.2013.01.006.

[10] P. Achten, T. van den Brink, J. Potma, M. Schellekens, and G. Vael, "A four-quadrant hydraulic transformer for hybrid vehicles," in *Proc. 11th Scandin. Int. Conf. Fluid Power*, Linköping, Sweden, Jun. 2009, pp. 324–339.

[11] P. Achten and T. van den Brink, "A hydraulic transformer with a swash block control around three axis of rotation," in *Proc. 8th Int. Fluid Power Conf.*, Dresden, Germany, Mar. 2012, pp. 134–148.
[12] J. Jiang and Z. Liu, "The experimental and CFD research on the pressure reduction process of the double rotor hydraulic transformer," *IEEE Access*, vol. 7, pp. 91569–91581, Jul. 2019, doi: 10.1109/ACCESS.2019.2926835.
[13] W. Shen, H. R. Karimi, and R. Zhao, "Comparative analysis of component design problems for integrated hydraulic transformers," *Int. J. Adv. Manuf. Technol.*, vol. 103, nos. 1–4, pp. 389–407, Jul. 2019, doi: 10.1007/s00170-019-03543-2.
[14] P. A. J. Achten, Z. Fu, and G. E. M. Vael, "Transforming Future Hydraulics: A New Design of a Hydraulic Transformer," in *Proc. 5th Scand. Int. Conf. Fluid Power*, Linköping, Sweden, 1997, p. 287ev.
[15] P. A. J. Achten, G. E. M. Vael, J. P. J. van den Oever, and Z. Fu, "'Shuttle' technology for noise reduction and efficiency improvement of hydrostatic machines," in *Proc. 7th Scand. Int. Conf. Fluid Power*. Berlin, Germany: Springer-Verlag, 2001, p. 269.
[16] C. Liu, Y. Liu, J. Liu, G. Yang, X. Zhao, and W. Quan, "Electro-hydraulic servo plate-inclined plunger hydraulic transformer," *IEEE Access*, vol. 4, pp. 8608–8616, Nov. 2016, doi: 10.1109/ACCESS.2016.2628355.
[17] P. A. J. Achten and Z. Fu, "Valving land phenomena of the innas hydraulic transformer," *Int. J. Fluid Power*, vol. 1, no. 1, pp. 39–47, Jan. 2000, doi: 10.1080/14399776.2000.10781081.
[18] X. P. Ouyang, B. Xu, and H. Y. Yang, "Innovation method of widening adjustable pressure range of hydraulic transformers," (in Chinese), *Chin. J. Mech. Eng.*, vol. 40, no. 9, pp. 28–32, Jan. 2004, doi: 10.3901/JME.2004.09.028.
[19] J. B. Hu, X. J. Li, and C. Wei, "A study on the transformation ratio characteristics of the hydraulic transformer," (in Chinese), *Trans. Beijing Inst. Technol.*, vol. 30, no. 2, pp. 167–169, Feb. 2010.
[20] C. Jing, J. Zhou, S. Yuan, and S. Zhao, "Research on the pressure ratio characteristics of a swash plate-rotating hydraulic transformer," *Energies*, vol. 11, no. 6, p. 1612, Jun. 2018, doi: 10.3390/en11061612.
[21] C. B. Jing, J. J. Zhou, and W. Wu, "Energy efficiency modeling and validation of a novel swash plate-rotating type hydraulic transformer," *Energy*, vol. 193, pp. 234–239, Dec. 2020, doi: 10.1016/j.energy.2019.116652.
[22] C.-M. Ning, Z.-Q. Chao, H.-Y. Li, and S.-S. Han, "Control performance and energy-saving potential analysis of a hydraulic hybrid luffing system for a bergepanzer," *IEEE Access*, vol. 6, pp. 34555–34566, Jun. 2018, doi: 10.1109/ACCESS.2018.2849215.
[23] J. H. Jiang and G. Z. Yang, "Development and research status of hydraulic transformer in hydraulic system," (in Chinese), *J. Chang'an Univ.*, vol. 36, no. 6, pp. 118–126, Nov. 2016.
[24] S. Lee and P. Y. Li, "Passivity based backstepping control for trajectory tracking using a hydraulic transformer," in *Proc. ASME/BATH Symp. Fluid Power Motion Control*, Chicago, IL, USA, Oct. 2015, pp. 1–10, doi: 10.1115/FPMC2015-9618.
[25] W. Shen and J. Wang, "Adaptive fuzzy sliding mode control based on pi-sigma fuzzy neutral network for hydraulic hybrid control system using new hydraulic transformer," *Int. J. Control, Autom. Syst.*, vol. 17, no. 7, pp. 1708–1716, Jul. 2019, doi: 10.1007/s12555-018-0593-9.
[26] W. Ronnie and J. O. Palmberg, "Hydraulic transformer in low-speed operation—A study of control strategies," in *Proc. Fluid Power. 5th JFPS Int. Symp.*, Nara, Japan, 2002, pp. 849–854.
[27] W. Shen, H. Huang, Y. Pang, and X. Su, "Review of the energy saving hydraulic system based on common pressure rail," *IEEE Access*, vol. 5, pp. 655–669, Jan. 2017, doi: 10.1109/ACCESS.2017.2648642.
[28] W. Shen, J. Jiang, X. Su, and H. R. Karimi, "A new type of hydraulic cylinder system controlled by the new-type hydraulic transformer," *Proc. Inst. Mech. Eng., C, J. Mech. Eng. Sci.*, vol. 228, no. 12, pp. 2233–2245, Aug. 2014, doi: 10.1177/0954406213515646.
[29] W. Shen, J. Wang, H. Huang, and J. He, "Fuzzy sliding mode control with state estimation for velocity control system of hydraulic cylinder using a new hydraulic transformer," *Eur. J. Control*, vol. 48, pp. 14–104, Jul. 2019, doi: 10.1016/j.ejcon.2018.11.005.
[30] G. Z. Yang, "Research on characteristics of variable hydraulic transformer and its flow distribution," Ph.D. dissertation, Harbin Inst. Technol., Harbin, China, 2019.
[31] Q. Q. Bao *et al.*, "Research on the low speed friction characteristic of hydraulic transformer," in *Proc. 11th Nat. Conf. Fluid Power Transmiss. Control*, Shanghai, China, 2020, pp. 1–6.
[32] J. J. Zhou, "Research on characteristics of rotate-plate hydraulic transformer," Ph.D. dissertation, Beijing Inst. Technol., Beijing, China, 2010.

QIANQIAN BAO received the B.S. degree in mechanical engineering from the Taiyuan University of Science and Technology, Taiyuan, China, in 2014, and the M.S. degree in mechanical engineering from Yanshan University, Qinhuangdao, China, in 2017. She is currently pursuing the Ph.D. degree in mechanical engineering with the Beijing Institute of Technology, Beijing, China. Her current research interests include hydraulic transmission and control, and fluid power components and systems.

JUNJIE ZHOU received the B.S. and Ph.D. degrees in mechanical engineering from the Beijing Institute of Technology, in 2009 and 2015, respectively.

From 2011 to 2013, he was a Visiting Scholar with the Maha Fluid Power Research Center of Purdue University. Since 2015, he has been an Assistant Professor with the Department of Mechanical Engineering, Beijing Institute of Technology. He is the author of one book and more than 40 journal or conference papers. His research interests include soft robotics and applications and fluid power components and systems. He is also a member of the Fluid Control Engineering Committee of the Chinese Society of Mechanics.

CHONGBO JING received the Ph.D. degree in mechanical engineering from the Beijing Institute of Technology, in 2010, where he is currently an Associate Professor with the School of Mechanical Engineering. His research interests include vehicle transmission theory and technology, and hydraulic transmission and control.

TIANRUI LI received the B.S. degree in mechanical engineering from the Harbin Institute of Technology, Weihai, China, in 2019. He is currently pursuing the M.S. degree in mechanical engineering with the Beijing Institute of Technology, Beijing, China. His current research interests include fluid power components and systems, and hydraulic transmission and control.

MIAOMIAO WANG received the B.S. degree in mechanical engineering from Chang'an University, Xi'an, China, in 2019. She is currently pursuing the M.S. degree in mechanical engineering with the Beijing Institute of Technology, Beijing, China. Her current research interest includes fluid power components and systems.